Dynamics of putative raft-associated proteins at the cell surface

Anne K. Kenworthy,[1,2,3] Benjamin J. Nichols,[1,4] Catha L. Remmert,[2] Glenn M. Hendrix,[2] Mukesh Kumar,[5] Joshua Zimmerberg,[5] and Jennifer Lippincott-Schwartz[1]

[1]Cell Biology and Metabolism Branch, National Institute of Child Health and Human Development,
 National Institutes of Health, Bethesda, MD 20895
[2]Department of Molecular Physiology and Biophysics and [3]Department of Cell and Developmental Biology,
 Vanderbilt University School of Medicine, Nashville, TN 37232
[4]Medical Research Council Laboratory of Molecular Biology, Cambridge CB2 2QH, England, UK
[5]Laboratory of Cellular and Molecular Biophysics, National Institute of Child Health and Human Development,
 National Institutes of Health, Bethesda, MD 20817

The Journal of Cell Biology

Lipid rafts are conceptualized as membrane microdomains enriched in cholesterol and glycosphingolipid that serve as platforms for protein segregation and signaling. The properties of these domains in vivo are unclear. Here, we use fluorescence recovery after photobleaching to test if raft association affects a protein's ability to laterally diffuse large distances across the cell surface. The diffusion coefficients (D) of several types of putative raft and nonraft proteins were systematically measured under steady-state conditions and in response to raft perturbations. Raft proteins diffused freely over large distances (>4 μm), exhibiting Ds that varied 10-fold. This finding indicates that raft proteins do not undergo long-range diffusion as part of discrete, stable raft domains. Perturbations reported to affect lipid rafts in model membrane systems or by biochemical fractionation (cholesterol depletion, decreased temperature, and cholesterol loading) had similar effects on the diffusional mobility of raft and nonraft proteins. Thus, raft association is not the dominant factor in determining long-range protein mobility at the cell surface.

Introduction

Biological membranes contain regions of lateral inhomogeneity known as microdomains (Maxfield, 2002; Edidin, 2003). The most studied class of putative microdomains are cholesterol and glycosphingolipid-enriched lipid rafts. These domains are thought to act as platforms with which proteins can selectively associate, leading to their lateral segregation (Simons and Ikonen, 1997; Simons and Toomre, 2000; Maxfield, 2002; Edidin, 2003). Proteins recovered in buoyant, detergent-resistant membrane (DRM) fractions after extraction of cells with certain detergents are commonly defined as raft associated. These proteins include glycosylphosphatidylinositol (GPI)-anchored proteins, acylated proteins, and a subset of transmembrane proteins (Simons and Ikonen, 1997; Brown and London, 1998a). Caveolae, a subset of lipid rafts, are additionally enriched in the protein caveolin (Rothberg et al., 1992). Lipid rafts are proposed to function in a large number of cellular functions ranging from protein and lipid sorting during post-Golgi sorting and endocytosis to regulation of cell signaling and viral entry and budding (Simons and Ikonen, 1997; Simons and Toomre, 2000; Ikonen, 2001; Edidin, 2003; Hancock, 2003). Despite this, a consensus view of the structure and dynamics of lipid rafts has yet to emerge (for review see Anderson and Jacobson, 2002; Maxfield, 2002).

One area of widespread interest is how rafts affect a protein's ability to laterally diffuse across cell membranes. In model membranes, the lateral mobility of lipids in a liquid-ordered phase is slower than in a liquid-disordered phase (Brown and London, 1998b; Korlach et al., 1999; Dietrich et al., 2002; Kahya et al., 2003). Indeed, several studies suggest

Abbreviations used in this paper: CTXB, cholera toxin B subunit; D, diffusion coefficient; DRM, detergent-resistant membrane; GPI, glycosylphosphatidylinositol; MβCD, methyl β-cyclodextrin; M_f, mobile fraction; NPC, Niemann-Pick type C; NRK, normal rat kidney; TX-100, Triton X-100.

Figure 1. **Models for lipid raft dynamics and protein diffusional mobility.** Models for diffusional mobility of lipid rafts (yellow), raft-associated proteins (red), and nonraft proteins (blue). (1) Stable, immobile rafts. Hypothetical barriers to lipid raft diffusion are depicted by the red lines. (2) Stable, mobile rafts. (3) Dynamic partitioning of raft proteins. (4) No rafts. For simplicity, putative barriers to individual protein diffusion are not depicted. See text for further details.
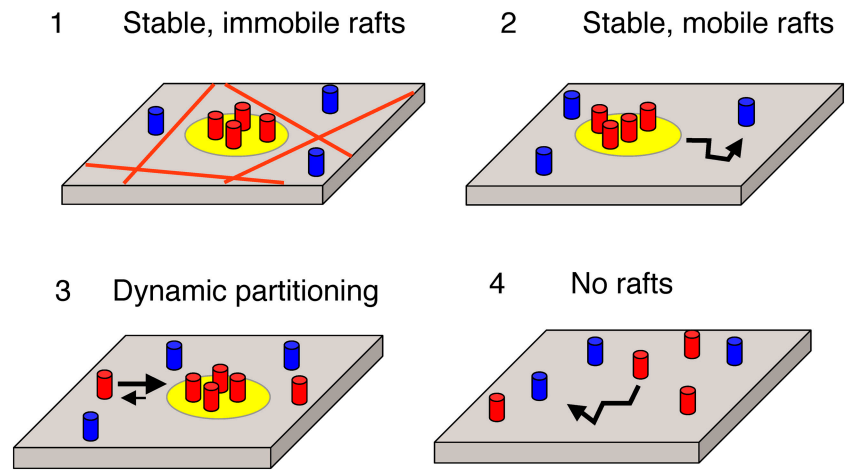
proteins and lipids undergo constrained and/or slowed diffusion within rafts (Sheets et al., 1997; Jacobson and Dietrich, 1999; Schütz et al., 2000; Niv et al., 2002; Shvartsman et al., 2003). Other measurements imply that raft proteins are stably associated over minutes with discrete domains, which themselves can either diffuse across the cell surface (Pralle et al., 2000) or are immobile, such as cell surface caveolae (Pelkmans et al., 2001; Thomsen et al., 2002). However, individual raft proteins do not appear to undergo correlated diffusion with one another (Vrljic et al., 2002), and the GPI-anchored protein CD59 shows similar behavior to a nonraft lipid in single molecule tracking studies (Subczynski and Kusumi, 2003). Thus, conflicting evidence exists as to whether raft domains are mobile or immobile structures, if protein associations with rafts are stable or transient, or how perturbations of raft structure affect the dynamics of individual proteins.

The relative importance of raft association compared with other factors known to modulate protein diffusional mobility is also uncertain. The lateral diffusion of proteins is typically 10–100-fold slower in cell membranes than in model membrane systems, even for lipid-binding proteins such as cholera toxin B subunit (CTXB; Bacia et al., 2002). In addition to the presence of membrane microdomains, several factors may contribute to the slowing of protein diffusion within biological membranes, including cytoskeletal barriers, interactions between protein ectodomains, and molecular crowding (Sheets et al., 1995; Edidin, 1996; Kusumi and Sako, 1996; Saxton, 1999; Lippincott-Schwartz et al., 2001). However, many of the studies defining these barriers to diffusion were performed before the development of the lipid raft model, and the role of lipid rafts in regulating membrane protein diffusion has not been systematically investigated.

We have measured the cell surface diffusion of putative raft-associated proteins tagged with GFP using FRAP. FRAP has been used extensively to characterize protein and lipid diffusional mobility and the domain structure of the plasma membrane, typically by monitoring recoveries into small spots ($\sim$1 µm; Edidin, 1994). In our experiments, we bleached and monitored protein recovery into an area of the membrane much larger than the proposed size of lipid raft domains. In these measurements, diffusional recovery would require either the diffusion of entire rafts or the diffusion of individual proteins outside of raft domains. We tested several models for the stability and organization of lipid raft domains by comparing the diffusional mobility of several kinds of raft proteins (glycolipid-binding, transmembrane, GPI-anchored, acylated, and prenylated proteins). We also examined the effects of cholesterol depletion, cholesterol loading, and reduced temperature on protein mobility. Our results indicate that putative raft-associated proteins are freely mobile and do not diffuse as part of discrete, stable domains across the cell surface. We also find that perturbations reported to affect lipid rafts have similar effects on the diffusional mobility of raft and nonraft proteins. This finding further indicates that raft association is not the dominant factor in determining protein mobility at the cell surface. Thus, if raft domains exist, raft proteins must rapidly partition into and out of them. Alternatively, raft domains may not be a significant feature of the cell surface under steady-state conditions.

Results

Models for lipid raft dynamics tested in this paper

To understand the properties of lipid rafts, we considered four simple models for how "raft" proteins might diffuse across the cell surface (Fig. 1). In model 1, lipid rafts are relatively stable, immobile structures, similar to caveolae (Pelkmans et al., 2001; Thomsen et al., 2002). In this model, rafts are unable to diffuse and proteins associate with rafts for long times. This predicts that raft proteins should exhibit low mobile fractions (M_f) and/or very slow diffusion coefficients (D_s). In model 2, rafts diffuse as stable entities across the cell surface (Pralle et al., 2000). A lipid raft domain itself should in principle be able to diffuse across the cell surface. Under conditions where viscosity is limiting, lateral diffusion varies inversely with the logarithm of the radius of the transmembrane portion of the diffusing species (Saffman and Delbrück, 1975). In a hop diffusion model where the membrane is compartmentalized by cytoskeletal corrals, long-range diffusion would be highly sensitive to size (Kusumi and Sako, 1996; Subczynski and Kusumi, 2003). In either case, this model predicts that the diffusion of raft domains of comparable dimensions will be independent of their protein constituents. So, different raft proteins should
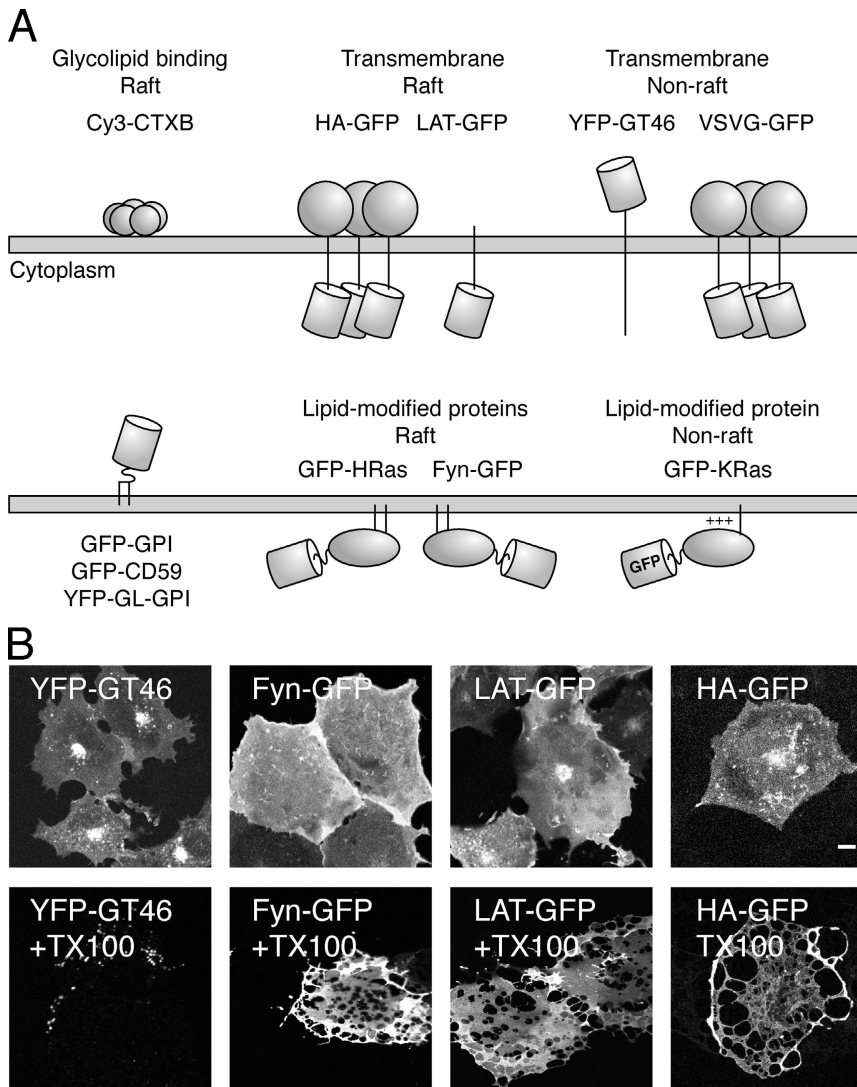
A

B

Figure 2. **Proteins used in this work.** (A) Membrane topology of GFP/YFP chimeras and fluorescently labeled toxin used in this work. The barrel indicates the position of the GFP. (B) Extraction of COS-7 cells grown on coverslips with 1% TX-100 at 4°C confirms that Fyn-GFP, LAT-GFP, and HA-GFP are present in DRM. YFP-GT46, a nonraft protein, is essentially completely solubilized under identical conditions. Bar, 10 μm.

exhibit similar Ds. In model 3, dynamic partitioning of raft proteins into and out of lipid raft domains occurs (Sheets et al., 1997; Jacobson and Dietrich, 1999; Schütz et al., 2000; Dietrich et al., 2002; Niv et al., 2002; Shvartsman et al., 2003). This partitioning would permit proteins to transiently populate raft domains as well as to undergo diffusion outside of rafts. D for any given protein should reflect the average of the diffusion within these two environments, which in turn depends on the protein's partitioning coefficient for rafts, the fraction of raftlike membrane, and other barriers to protein diffusion that exist in the raft and nonraft domains. In model 4, raft proteins diffuse independently of one another due to the absence of significant raft domains. In this model, lipid raft domains by themselves make a nominal contribution to protein diffusion. Instead, each protein experiences its own distinct set of constraints to its diffusion, giving rise to different Ds for different proteins.

Protein markers for raft and nonraft domains

To test these various models, we examined the diffusional mobility of plasma membrane proteins tagged with the fluorescent proteins GFP or YFP. We examined a number of different proteins in our work to test how the properties of raft proteins compare with one another as well as with nonraft proteins (Fig. 2 A). Proteins were chosen based on previous biochemical fractionation studies identifying them as either raft-associated or nonraft (Skibbens et al., 1989; Scheiffele et al., 1997; Orlandi and Fishman, 1998; Zhang et al., 1998b; Pralle et al., 2000; Keller et al., 2001; Nichols et al., 2001; Prior et al., 2001; Niv et al., 2002). The raft proteins studied include two transmembrane proteins (HA-GFP and LAT-GFP), three GPI-anchored proteins (GFP-GPI, YFP-GL-GPI, and GFP-CD59), and two cytoplasmically oriented proteins (Fyn-GFP and GFP-HRas). Transient expression of CFP/YFP-GPI causes a fivefold increase in the total amount of GPI anchors in COS-7 cells (Glebov and Nichols, 2004). As a marker for raft lipids, we labeled cells with fluorescently tagged CTXB (Cy3-CTXB). Nonraft proteins used as negative controls included two transmembrane proteins, VSVG-GFP and YFP-GT46 (also known as LYFPGT46), and a cytoplasmically oriented protein, GFP-KRas. As an internal control, we compared two versions of VSVG-GFP that vary only in the linker region (Toomre et al., 1999; Keller et al., 2001). Control experi-
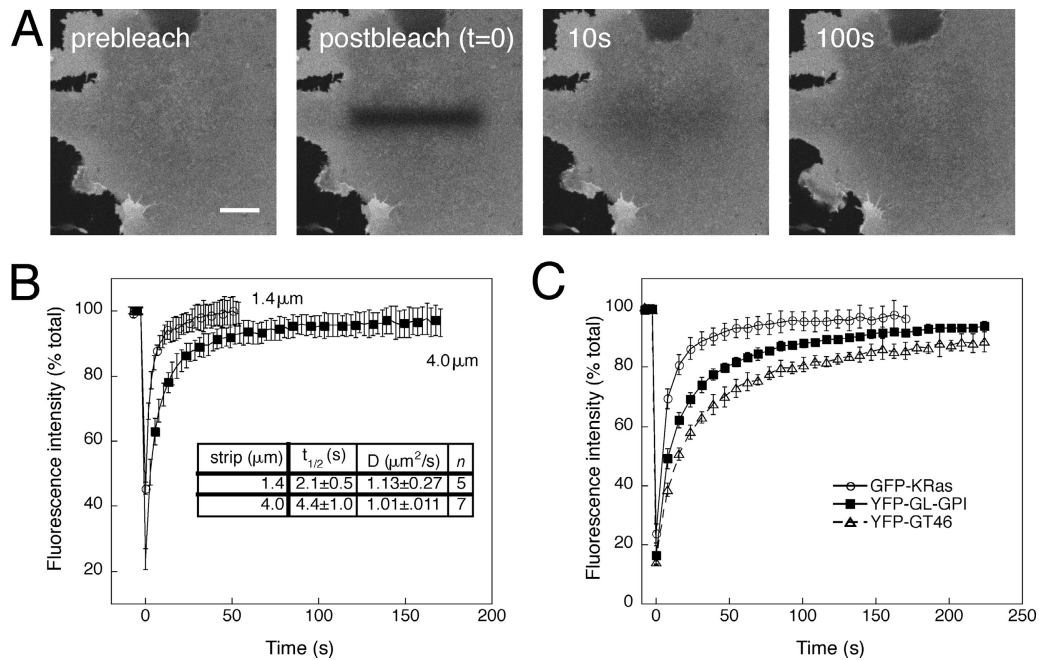
Figure 3.   **Large-scale lateral diffusion measurements by confocal microscopy.** (A) Selected images from a confocal FRAP experiment at 37°C of GFP-KRas expressed in COS-7 cells. Bleach box, 4 μm wide. Bar, 10 μm. (B) Kinetics of recovery for 1.4- (circles) versus 4-μm-wide (squares) bleach box. Calculated D and $t_{1/2}$ values are indicated. Data shown are for GFP-KRas expressed in COS-7 cells at 37°C. (C) Kinetics of recovery for YFP-GT46 (triangles), YFP-GL-GPI (squares), and GFP-KRas (circles) in COS-7 cells at 37°C using a 4-μm-wide bleach box. Each curve shows the mean ± SD from seven to nine cells from a single experiment. The calculated Ds were as follows: GFP-KRas, 1.01 ± 0.11 μm²/s; YFP-GL-GPI, 0.47 ± 0.07 μm²/s; YFP-GT46, 0.23 ± 0.02 μm²/s.

ments verified that upon extraction of cells grown on coverslips with 1% ice-cold Triton X-100 (TX-100), putative raft proteins were largely present in the DRM remnants, whereas nonraft proteins were efficiently solubilized (Fig. 2 B and not depicted). These observations are consistent with previous biochemical experiments based on the low buoyant density of DRMs.

Large-scale diffusional mobility assay measured by confocal FRAP

To measure the diffusional mobility of raft-associated proteins, we used a variation on FRAP, confocal FRAP (Ellenberg et al., 1997; Zaal et al., 1999; Nehls et al., 2000). In these experiments, we monitored fluorescence of the protein of interest using low-intensity laser excitation. A defined region was photobleached using high-intensity light by transiently increasing the laser power, and the diffusive exchange of bleached proteins with nearby unbleached molecules was then followed (Fig. 3 A). Recovery into the bleached region can be described by two parameters, an apparent D and M_f (Edidin, 1994; Lippincott-Schwartz et al., 2001). D provides a measure of how fast recovery occurs, whereas M_f reports the fraction of fluorescent molecules that are able to recover into the bleached area over the time course of the experiment.

To detect possible diffusion of raft domains themselves as well as the diffusion of individual proteins, the bleached region used, a strip 4 μm wide, was much larger than the proposed size of lipid rafts (0–700 nm in diameter; Anderson and Jacobson, 2002). Such large-scale measurements are also of interest because experiments visualizing DRM suggest

lipid rafts comprise a significant fraction of the plasma membrane (Mayor and Maxfield, 1995; Kenworthy and Edidin, 1998; Hao et al., 2001; Nichols et al., 2001). Recoveries in a strip this size occurred over tens of seconds, allowing us to readily quantitate recovery into the bleached region while collecting images of the surrounding area.

Control experiments verified that fluorescence recovery had the characteristics of lateral diffusion. Recovery did not occur in samples fixed with 3.7% PFA (unpublished data). We also confirmed that the characteristic recovery time was proportional to the size of the bleached region, as expected for a protein undergoing lateral diffusion. To test this, we compared recoveries for a given protein into two different size bleach boxes (Fig. 3 B). Recovery was faster in the smaller bleach box, yet identical Ds were obtained for both and were well described by the simulation data for diffusive recoveries (unpublished data). Although dimerization of GFP-tagged membrane proteins has been observed by FRET (Zacharias et al., 2002), introduction of point mutations to eliminate dimerization had no detectable effect on lateral diffusion (unpublished data).

To compare the diffusional mobility of different proteins, we performed FRAP experiments using identically sized bleach boxes. Under these conditions, differences in the kinetics and extent of recovery will reflect the diffusional mobility of the individual proteins. Recovery curves for a population of cells expressing a given protein were similar, but differences in the kinetics of recovery were apparent between proteins (Fig. 3 C). Only a small fraction of proteins were immobile, as M_f was typically >85% (Fig. 3 C). In contrast, caveolin-1-GFP was nearly 100% immobile (unpublished data).
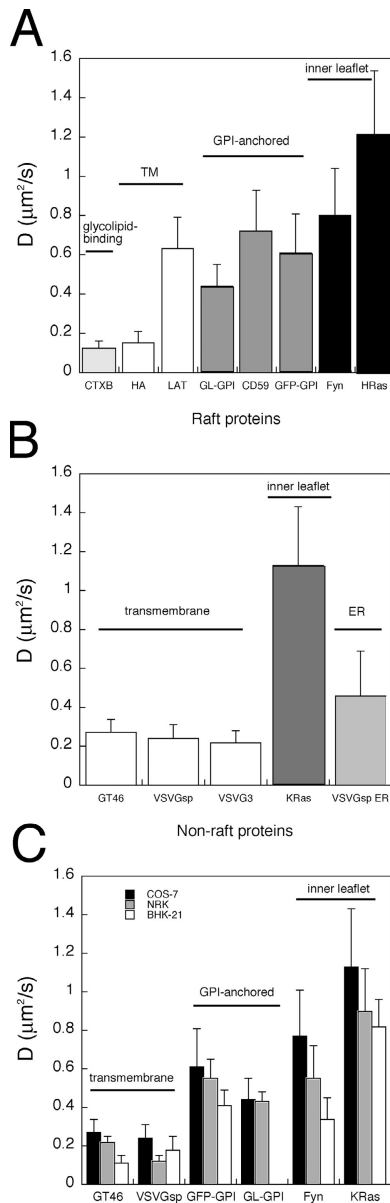
Figure 4. **Diffusional mobilities of raft and nonraft proteins at the cell surface at 37°C**. D for raft proteins (A) and for nonraft proteins (B) in COS-7 cells. (C) D for a subset of proteins in COS-7, BHK-21, and NRK cells. The bleach box was 4 μm wide in COS-7 cells and 1.4 μm wide in NRK and BHK-21 cells. Error bars are the mean ± SD.

Table I. **Percent mobile fractions of raft and nonraft proteins in large-scale diffusion measurements in COS-7 cells**

Protein	Treatment			
	37°C	**MβCD**	**20°C**	**10°C**
Raft				
Cy3-CTXB	81 ± 8 (40)	76 ± 7 (29)	66 ± 8 (32)	
HA-GFP	75 ± 10 (15)			
LAT-GFP	89 ± 6 (26)		90 ± 9 (19)	86 ± 4 (6)
GFP-GPI	93 ± 5 (27)	93 ± 7 (14)	87 ± 6 (20)	79 ± 7 (4)
GFP-CD59	92 ± 5 (17)			
YFP-GL-GPI	91 ± 7 (46)	90 ± 3 (12)		
Fyn-GFP	93 ± 8 (41)	93 ± 4 (20)	83 ± 4 (11)	84 ± 6 (5)
GFP-HRas	95 ± 5 (32)			
Nonraft				
YFP-GT46	91 ± 7 (27)	89 ± 6 (12)	81 ± 5 (21)	67 ± 13 (4)
GFP-VSVGsp	88 ± 8 (45)	70 ± 10 (7)		
GFP-VSVG3	85 ± 4 (17)			
GFP-KRas	93 ± 7 (27)		92 ± 4 (11)	88 ± 14 (8)

Values for treatment represent the mean ± SD. The numbers in parentheses represent n.

GFP-GPI (t test, P < 0.001). Raft proteins localized to the inner leaflet of the plasma membrane, Fyn-GFP and GFP-HRas, exhibited the most rapid diffusion, similar to values recently reported for GFP-HRas by spot photobleaching (Niv et al., 2002).

For comparison, we measured the diffusional mobility of nonraft proteins (Fig. 4 B). Like the raft proteins, all of the nonraft proteins examined showed recoveries characteristic of lateral diffusion, with M_f > 90% (Table I). D for VSVG3-sp-GFP and VSVG3-GFP were identical to one another and similar to that obtained for YFP-GT46. These values are in good agreement with the D of 0.13 μm²/s for VSVG3-sp-GFP at 32°C measured from the diffusional spread of the protein at the cell surface upon vesicle fusion (Toomre et al., 2000). D for VSVG-GFP is somewhat slower at the plasma membrane than in the ER (Fig. 4 B; Nehls et al., 2000). D for GFP-KRas was extremely fast and similar to that of GFP-HRas. To confirm these findings, we repeated measurements for selected proteins in two other cell types (Fig. 4 C) and obtained similar results. Together, these data indicate that raft proteins are highly mobile and are able to diffuse across the cell surface as rapidly as nonraft proteins. However, raft proteins differ significantly in their diffusional mobilities, a result that could be explained by either the dynamic partitioning or the no raft model (Fig. 1).

Lower temperatures slow both raft and nonraft protein diffusion

Raft proteins partition into DRMs more efficiently at 4°C than 37°C (Brown and Rose, 1992; Cerneus et al., 1993), and the formation of raft domains is driven by lowered temperature in model membranes (Dietrich et al., 2001a,b; Samsonov et al., 2001). We tested whether or not at decreased temperatures, in which DRM association is enhanced (Fig. 5 A), we could observe any evidence for increased partitioning of raft proteins into domains by FRAP. D was lowered by approximately twofold at 20°C for both raft and nonraft pro-

Diffusional mobility for raft and nonraft proteins under steady-state conditions

Next, we used the confocal FRAP assay to compare the diffusional mobility of raft proteins with one another. For all the proteins examined, we observed recoveries characteristic of lateral diffusion, with high M_f (Table I). CTXB is internalized over time, and the endosomal fraction of the protein is unable to recover rapidly after a photobleach, giving rise to an effective immobile fraction (Table I). D varied significantly for different raft proteins, ranging from 0.1 to 1.2 μm²/s at 37°C (Fig. 4 A). The slowest recoveries were observed for Cy3-CTXB and HA-GFP. D was higher for the three GPI-anchored proteins and LAT-GFP, but was significantly slower for YFP-GL-GPI than for GFP-CD59 and
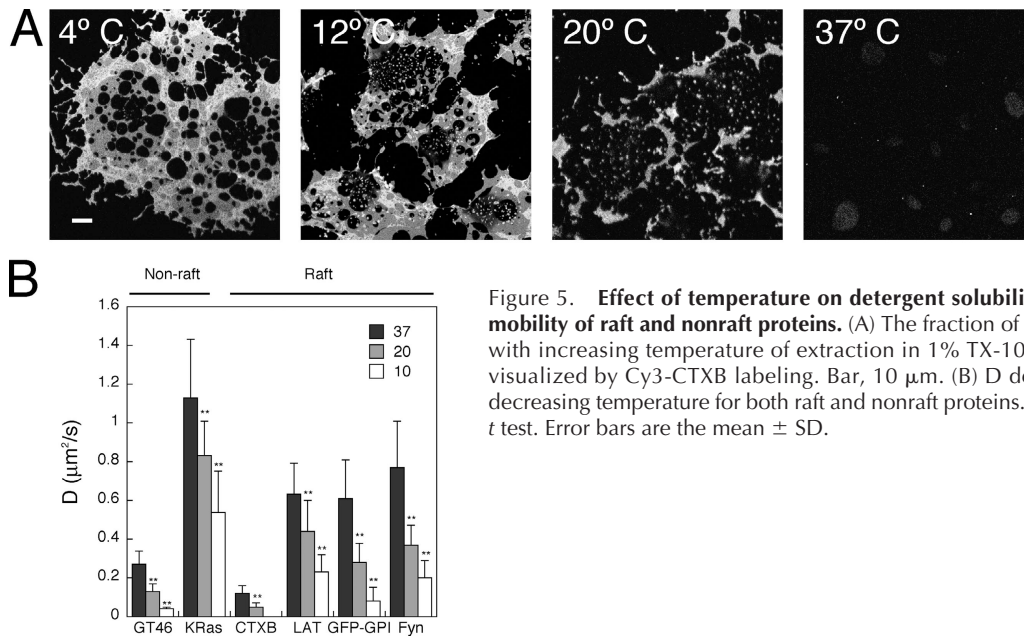
Figure 5. **Effect of temperature on detergent solubility and lateral mobility of raft and nonraft proteins.** (A) The fraction of DRM decreases with increasing temperature of extraction in 1% TX-100. DRM was visualized by Cy3-CTXB labeling. Bar, 10 μm. (B) D decreases with decreasing temperature for both raft and nonraft proteins. **, P < 0.0001, *t* test. Error bars are the mean ± SD.

teins and showed further decreased mobility at 10°C (Fig. 5 B). A similar effect was observed for VSVG-GFP in the ER (Reits and Neefjes, 2001; unpublished data), suggesting that this phenomenon reflects a general effect on membrane viscosity throughout the cell. These results are consistent with previous measurements showing that protein and lipid diffusion at the plasma membrane is temperature dependent (Wey et al., 1981; Hillman and Schlessinger, 1982; Jacobson et al., 1984; Aroeti and Henis, 1988) but do not show a simple correlation with raft domains.

Figure 6. **Effect of cholesterol depletion on detergent solubility and lateral mobility of raft and nonraft proteins, and quantitation of filipin staining after perturbations in cellular cholesterol levels.** (A) Cholesterol depletion enhances the TX-100 solubility of YFP-GL-GPI and Cy3-CTXB. A similar effect was observed for other raft proteins (not depicted). Bar, 10 μm. (B) Cholesterol depletion slows the diffusion of raft and nonraft proteins at 37°C. Cells were pretreated with 10 mM MβCD for 30 min at 37°C before TX-100 extraction or FRAP measurements. **, P < 0.0001; *, P < 0.01, *t* test. Error bars are the mean ± SD. (C) Quantitation of cholesterol by filipin staining. This method, although not strictly quantitative (Severs, 1997; Maxfield and Wüstner, 2002), provides a qualitative estimate of the cholesterol levels. Filipin staining was performed on fixed cells and quantified from images obtained using a CCD camera for identical exposure times as described in Materials and methods. Data are shown from a representative experiment. Error bars are the mean ± SD. All treatments are significantly different than controls (P < 0.0001, *t* test).
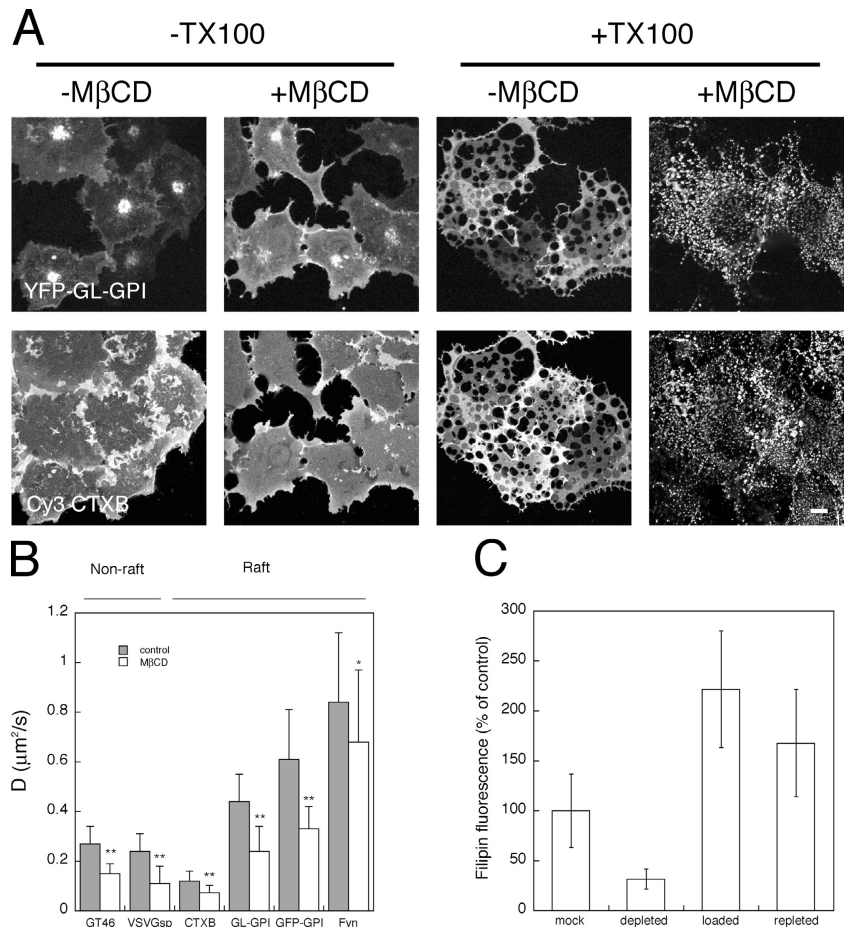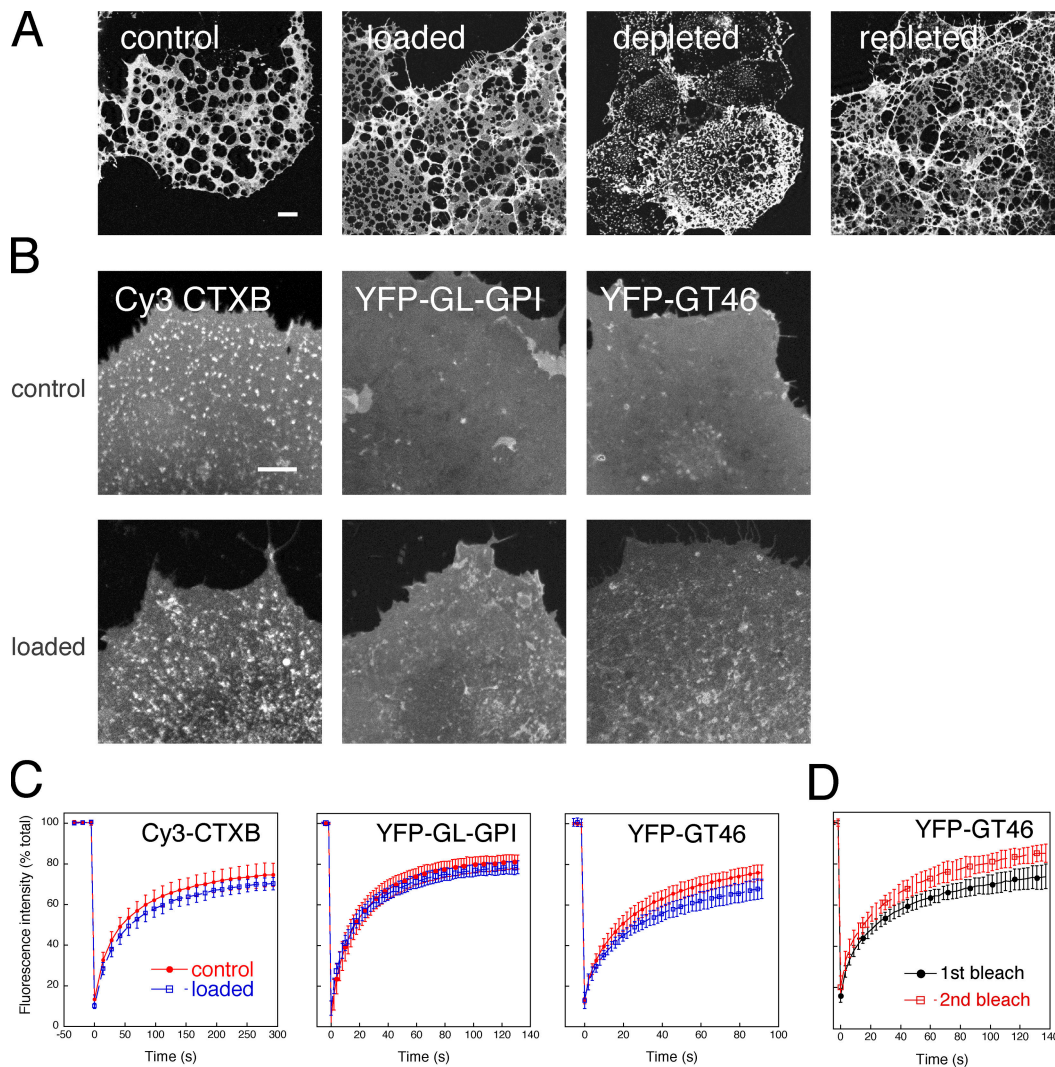
Figure 7. **Effect of cholesterol loading on detergent solubility, cell surface distribution, and lateral mobility of raft and nonraft proteins.**
(A) Comparison of DRM in mock-treated, cholesterol-loaded, cholesterol-depleted, and cholesterol-repleted cells. DRM were visualized by Cy3-CTXB labeling. Bar, 10 μm. (B) Effect of cholesterol loading on the cell surface distribution of raft (Cy3-CTXB and YFP-GL-GPI) and nonraft (YFP-GT46) proteins in living cells. Averaged prebleach images from confocal FRAP experiments are shown for control and cholesterol-loaded cells. Bar, 10 μm. (C) Effect of cholesterol loading on diffusional mobilities of raft proteins and nonraft proteins. Recovery curves show the mean ± SD from 7–11 cells from a representative experiment for control (red circles) versus cholesterol-loaded (blue squares) cells at 22°C. (D) Repetitive bleaching of YFP-GT46 in cholesterol-loaded cells to test for the presence of an immobile pool of protein. After performing a FRAP measurement on a given cell (first bleach, black circles), a second measurement was made using exactly the same bleach box (second bleach, red squares). Recovery curves show the mean ± SD from 7–11 cells from a representative experiment at 22°C.

Cholesterol depletion with methyl-β-cyclodextrin (MβCD) slows both raft and nonraft protein diffusion

Cholesterol is thought to play a pivotal role in the formation and stabilization of lipid rafts (Brown and London, 1998b; Rietveld and Simons, 1998; Simons and Ehehalt, 2002). The dynamic partitioning model predicts raft association selectively slows protein diffusion, and thus cholesterol depletion should increase the mobility of raft proteins. To test this prediction, we used MβCD to acutely deplete cholesterol from cells (Simons and Toomre, 2000). DRM remnants in cholesterol-depleted cells were substantially smaller that those observed in mock-treated cells (Fig. 6 A), and cholesterol levels were reduced to ~30% of control by MβCD treatment as detected by filipin staining (Fig. 6 C). Remarkably, D for both raft and

nonraft markers was significantly reduced (approximately twofold) upon cholesterol depletion, with no change in M_f (Table I and Fig. 6 B). These findings are inconsistent with the notion that the principle effect of acute cholesterol depletion is to release proteins from lipid rafts. They further indicated that MβCD's effects are not specific to raft proteins.

Cholesterol loading shifts the subcellular distribution of cell surface proteins but has little effect on protein mobility

The effects of excess cholesterol on the properties of lipid rafts in cell membranes have been largely unexplored (Tabas, 2002). However, in a model membrane system, cholesterol addition increases the size of cholesterol-enriched domains,

Table II. **Percent mobile fraction of raft and nonraft proteins in cholesterol-loaded COS-7 cells at 22°C**

Protein	Treatment			
	Control	Loaded	Rebleach$_{control}$	Rebleach$_{loaded}$
Cy3-CTXB	66 ± 8 (23)	64 ± 8 (22)		
YFP-GL-GPI	77 ± 7 (27)	72 ± 6[a] (27)		
YFP-GT46	79 ± 5 (28)	69 ± 12[a] (29)	80 ± 8 (30)	79 ± 9 (30)

Values for treatment represent the mean ± SD. The numbers in parentheses represent n.
[a]$P < 0.05$ compared to control, t test.

eventually leading to a continuous raftlike phase (Kahya et al., 2003; Lawrence et al., 2003). Assuming the same occurs in cell membranes, the partitioning model would predict a decrease in D of raft proteins due to enhanced partitioning into raft domains, accompanied by immobilization of nonraft proteins due to their exclusion from increasingly large raft domains. To test these predictions, we used water-soluble cholesterol (MβCD–cholesterol complexes) to introduce cholesterol into the plasma membrane (Christian et al., 1997; Lange et al., 1999; Feng et al., 2003). Loading cells with approximately twofold higher cholesterol levels than in mock-treated cells (Fig. 6 C) did not substantially change the morphology of DRM remnants (Fig. 7 A).

FRAP recovery curves for Cy3-CTXB, YFP-GL-GPI, and YFP-GT46 yielded similar halftimes in control and cholesterol-loaded cells, whereas M_f of YFP-GL-GPI and YFP-GT46 were significantly decreased (Fig. 7 C, Table II, and not depicted). Cholesterol loading also caused the accumulation of YFP-GT46, and to a lesser extent YFP-GL-GPI, in patchy and/or punctate structures (Fig. 7 B). These punctate structures appeared to represent an endocytosed pool of protein based on two findings. First, immunofluorescence labeling experiments using anti-GFP antibodies showed that the YFP-GT46–positive structures were inaccessible to labeling in nonpermeabilized cells (unpublished data). Second, the punctate structures did not recover over short time periods, as expected for a vesicular pool. By performing a second bleach of the same region of interest in cholesterol-loaded cells, an increased M_f of YFP-GT46 was observed as a result of eliminating this intracellular immobile fraction (Fig. 7 D and Table II). This observation suggested that the effects of cholesterol loading on the apparent diffusional mobility of YFP-GT46 are due to the redistribution of the protein to an intracellular pool rather than altered lateral mobility within the membrane. Thus, cholesterol addition to cell membranes does not have effects analogous to those observed in model membrane systems. However, loading does appear to increase the extent of protein internalization.

Discussion

Raft proteins are mobile and do not diffuse as part of stable structures

In this work, we used FRAP to investigate the dynamic properties of lipid rafts and the overall effect of lipid rafts on protein diffusional mobility. In our experiments, we mea-

sured recoveries in an area much larger than the proposed size of lipid rafts to monitor possible diffusion of raft domains themselves as well as diffusion of proteins outside of raft domains. Our data revealed that raft proteins are able to diffuse large distances across the cell membrane and that they have high M_f. Yet, D for individual raft proteins varied over an order of magnitude depending on the protein examined (Fig. 4). These results are incompatible with two of the models for lipid raft structure and dynamics described in Fig. 1. The first is the stable, immobile raft model. Except for the specialized case of caveolin (Pelkmans et al., 2001; Thomsen et al., 2002), this model is not generally consistent with the behavior of raft proteins as observed in our experiments. The second model, implied by photonic force microscopy measurements (Pralle et al., 2000), is one in which rafts diffuse as stable entities across the cell surface. Arguing against this model are two findings: those here showing the lack of correlation in Ds of different raft proteins and previous data from single molecule tracking showing that individual raft proteins diffuse independently of one another (Vrljic et al., 2002).

Diffusional mobility is more strongly correlated with membrane anchorage than with raft association

Our finding that Ds varied tenfold for different raft proteins is consistent with previous observations showing that a variety of barriers to protein diffusional mobility exist in cell membranes (Sheets et al., 1995; Edidin, 1996; Kusumi and Sako, 1996; Saxton, 1999; Lippincott-Schwartz et al., 2001). These results also indicate that raft association is not the dominant factor in determining the overall mobility of a particular protein, a possibility consistent with either the dynamic partitioning or no raft models (Fig. 1). Instead, we observed a correlation between protein diffusional mobility and the mode of membrane anchorage, with $D_{acylated\ or\ prenylated} > D_{GPI-anchored\ proteins} > D_{transmembrane}$ regardless of whether or not a particular protein is raft associated (Fig. 4).

The high mobility of GPI-anchored proteins has been previously noted and is thought to reflect the lipid-based anchor of these proteins (Ishihara et al., 1987; Edidin and Stroynowski, 1991) but is modulated by the ectodomain (Zhang et al., 1991). This finding could explain why we observed significantly higher Ds for GPI-anchored proteins than a transmembrane form of HA, in contrast to a recent report (Shvartsman et al., 2003). Until now, the diffusional properties of acylated and prenylated proteins have remained largely unexplored because of their inaccessibility to labeling with exogenous fluorescent probes. The high Ds of these proteins suggest that their lipid anchors facilitate their relatively free diffusion and/or that the microenvironment of the inner leaflet contains fewer barriers to protein diffusion than the outer leaflet where GPI-anchored proteins are found.

LAT-GFP and Cy3-CTXB are two exceptions to the correlation between D and membrane anchorage (Fig. 4). We speculate that, given the effective absence of an ectodomain (Zhang et al., 1998a), LAT is more directly comparable to proteins localized to the inner leaflet of the plasma membrane than other transmembrane proteins. The slow diffusion of CTXB, a homo-pentamer, could potentially arise

from cross-linking and trapping other cell surface proteins that can interact with the cytoskeleton, similar to that proposed for cross-linked GPI-anchored proteins (Suzuki and Sheetz, 2001). Association of CTXB with immobile caveolae before its eventual internalization may also slow its diffusion.

The effects of reduced temperature and cholesterol depletion on protein diffusion are not limited to alterations of raft dynamics

To distinguish between the dynamic partitioning (Fig. 1, Model 3) and no raft domain (Fig. 1, Model 4) models, we first investigated the sensitivity of protein mobility to two conditions previously shown to alter partitioning of raft proteins into DRMs, temperature reduction and cholesterol depletion. We found that both temperature reduction and cholesterol depletion decreased the diffusional mobility of both raft and nonraft proteins to a similar extent (Figs. 5 B and 6 B). This observation does not completely eliminate the possibility of altered partitioning of raft proteins into rafts in response to these treatments, but indicates that other factors play a more dominant role in determining a protein's lateral mobility under these conditions. Interestingly, an immobilizing effect of cholesterol depletion also has been noted in a recent study of MHC-class I lateral mobility (Kwik et al., 2003). This effect was linked to changes in the organization of the actin cytoskeleton in response to MβCD treatment, which have also been noted in other studies (Grimmer et al., 2002; Hering et al., 2003; see also the retraction of cells during this treatment in Fig. 6 A). Given the potential connection between lipid rafts and the actin cytoskeleton (Maxfield, 2002), it is unclear if these effects occur in addition to, or as a consequence of, disruption of raft domains. Nevertheless, these findings raise questions about the specificity of acute cholesterol depletion on lipid domain structure/function and highlight the possibility that cytoskeletal reorganization might account for some of the observed functional effects of MβCD treatment.

Effects of cholesterol loading, another method to explore membrane domain structure and function on raft protein dynamics

To further attempt to distinguish the effect of raft perturbations on protein mobility, we used cholesterol loading. Given that major cellular defects are associated with conditions of aberrant cholesterol accumulation, such as hypercholesterolemia and Niemann-Pick type C (NPC) disease, understanding the effects of excess cholesterol on lipid raft structure and function is of physiological importance. Based on work in model systems (Kahya et al., 2003; Lawrence et al., 2003), we hypothesized that cholesterol loading should lead to the formation of additional lipid rafts and/or to an increase in size of existing rafts. However, little change in the halftime of recovery was seen for any of the proteins studied in cholesterol-loaded cells (Fig. 7). These data suggest that if cholesterol loading indeed increases the fraction of raftlike membrane, diffusion of raft proteins within this environment is not significantly slowed under these conditions. However, we did observe decreased M_f in response to cho-

lesterol loading. This effect appears to be due to enhanced endocytosis of proteins in response to cholesterol loading, potentially resulting from proteins being driven out of an expanded raft phase. The identity of these putative endocytic structures remains to be determined. Both clathrin-mediated and nonclathrin endocytic pathways are sensitive to membrane cholesterol levels (Rodal et al., 1999; Subtil et al., 1999; Nichols and Lippincott-Schwartz, 2001). Moreover, defects in the trafficking of glycolipids internalized by nonclathrin pathways have been correlated with the accumulation of excess cholesterol in multiple sphingolipid storage diseases including NPC (Puri et al., 1999). Our observations of continued CTXB uptake in cholesterol-loaded cells (Fig. 7 B) are in line with observations that CTXB is able to enter endocytic structures in NPC1-deficient cells (Sugimoto et al., 2001; Choudhury et al., 2002). It will be of interest to determine the nature of the trafficking defects induced by acute cholesterol loading and to discern if the mechanisms are similar to those observed in NPC-deficient cells.

Implications for models for lipid rafts

Our data indicate that raft association is not the major determinant of plasma membrane protein diffusional mobility under steady-state conditions. Thus, we can rule out several models for raft dynamics, including stable immobile rafts and stable mobile rafts, on the basis of our findings. It is possible that a small fraction of proteins are associated with stable immobile domains, as we observed an immobile fraction of 10–15% for the majority of the proteins examined (Table I). However, the absence of an effect of cholesterol depletion on the size of the immobile fractions that we and others (Lommerse et al., 2004) have detected, and the similar immobile fractions of raft and nonraft proteins, suggests that the immobile fraction is not generated by recruitment to lipid rafts. It is also possible that overexpression of our marker proteins may overwhelm and mask a small amount of behavior corresponding to models 1 or 2. However, diffusion of the raft marker GFP-HRas was previously shown to be independent of expression levels (Niv et al., 2002). Techniques with single molecule sensitivity such as fluorescence correlation spectroscopy could provide insight into this issue in the future.

Our findings also reveal that treatments shown to perturb the rafts detected in model membrane systems (cholesterol depletion, temperature reduction, and cholesterol addition) have effects on protein diffusion in cells that cannot be explained solely by predictions of the raft hypothesis. However, these treatments may give rise to pleiotropic effects that mask underlying changes in raft properties. Therefore, on the basis of our current data we cannot definitively distinguish between the dynamic partitioning model and the absence of detectable raft domains (Fig. 1). Interestingly, the predictions of the dynamic partitioning and no raft models converge under conditions where lipid rafts comprise a small fraction of the cell surface and proteins spend only a small amount of time visiting them, or if the fraction of raftlike membrane is normally large but protein diffusion within a raft is not very different than in nonraft regions of the membrane. Our understanding of how rafts function in vivo now needs to take into account the fact that incorporation into

biochemically defined rafts is not indicative of incorporation into stable microdomains in the plasma membrane.

Materials and methods

DNA constructs, cell transfections, and fluorescent probes

Unless otherwise indicated, all chemicals were obtained from Sigma-Aldrich. For simplicity, EGFP is referred to as GFP throughout. GFP-GPI and GFP-CD59 were as described previously (Nichols et al., 2001). GFP-HRas, GFP-KRas, and Fyn-GFP (Choy et al., 1999) were provided by M. Philips (New York University School of Medicine, New York, NY). LAT-GFP (Bunnell et al., 2002) was obtained from L. Samelson (National Institutes of Health, Bethesda, MD). YFP-GL-GPI (Keller et al., 2001), YFP-GT46 (Pralle et al., 2000), VSVG3-sp-GFP (Keller et al., 2001), and VSVG-3-GFP (Toomre et al., 1999) were provided by P. Keller and K. Simons (Max Planck Institute of Molecular Cell Biology and Genetics, Dresden, Germany). YFP-GT46 is an artificial secretory protein containing a signal sequence, YFP, a consensus N-glycosylation site, the transmembrane domain of the LDL receptor, and the cytoplasmic tail of CD46 (Pralle et al., 2000). To construct HA-GFP, the influenza hemagglutinin gene was PCR amplified from the plasmid pCB6HA (a gift from M.G. Roth, University of Texas Southwestern Medical Center, Dallas, TX) and cloned into the plasmid pEGFP-N1 (CLONTECH Laboratories, Inc.). In control experiments, constructs containing monomeric (Zacharias et al., 2002) forms of fluorescent protein were examined (mYFP-GL-GPI, mYFP-GT46, mCitFP-LAT, and VSVG-mYFP; Glebov and Nichols, 2004).

Cells were grown in DME (COS-7 and normal rat kidney [NRK] cells) or EMEM (BHK-21) supplemented with 10% FCS, glutamine, penicillin, and streptomycin (Biofluids). Transient transfections were performed using Fu-GENE 6 (Roche Molecular Biochemicals). CTXB was fluorescently labeled with Cy3 (Amersham Biosciences) as per the manufacturer's instructions and was used at a final concentration of 1 μg/ml.

Fluorescence microscopy and diffusional mobility measurements

Filipin fluorescence was imaged using a wide field microscope (model Axiophot; Carl Zeiss MicroImaging, Inc.). Fluorescence was excited with a mercury arc lamp, and emission was detected using a DAPI filter set. Images were collected using a 40× 1.3 NA Plan-Neofluar objective (Carl Zeiss MicroImaging, Inc.) and captured using a MicroMax CCD camera (Princeton Instruments) and MetaMorph acquisition software. Images were obtained using identical exposure times for cells subjected to various treatments in each experiment. Quantitation of filipin fluorescence was performed using NIH Image.

All other fluorescence images were obtained using a confocal microscope (model LSM 510; Carl Zeiss MicroImaging, Inc.). Fluorescence emission resulting from 488-nm excitation for GFP, 488- or 514-nm excitation for YFP, and 543-nm excitation for Cy3 was detected using filter sets supplied by the manufacturer. Cells were held at 37°C on the microscope stage unless otherwise indicated. For FRAP measurements, a 40× 1.3 NA Plan-Neofluar objective or 100× 1.4 NA Plan-Apochromat objective (Carl Zeiss MicroImaging, Inc.) was used with the confocal pinhole set at 1–2 Airy units. Photobleaching of GFP, YFP, or Cy3 was performed using 5–20 scans with the 488-nm laser line at full power in a rectangular region of interest 4 μm wide (COS-7 cells) or 1.4 μm wide (BHK-21 and NRK cells). Pre- and postbleach images were monitored at low laser intensity. Fluorescence recoveries in the bleached region and overall photobleaching in the whole cell during the time series were quantitated using the LSM software (Carl Zeiss MicroImaging, Inc.). Photobleaching of Cy3 did not induce photodamage to the membrane, as evidenced by control experiments showing identical recoveries for GFP-HRas in cells labeled with Cy3-CTXB versus unlabeled CTXB. For presentation purposes, LSM 510 images were exported in TIFF format and their contrast and brightness optimized in Photoshop.

Ds were calculated from the photobleaching data using Diffuse, a program that simulates diffusive recovery into the bleached region using the series of images collected after the photobleaching episode (Ellenberg et al., 1997; Zaal et al., 1999; Nehls et al., 2000; Siggia et al., 2000; program available upon request). LSM 510 images were exported in TIFF format and converted to PPM format for analysis with the Diffuse program. Statistical differences were evaluated using the t test. M_f was calculated as described previously (Ellenberg et al., 1997).

TX-100 extraction

TX-100 extractions were performed as described previously (Nichols et al., 2001) except that cells were incubated in TX-100 for 15 min and after fixa-

tion subsequently labeled with Cy3-CTXB before imaging. Where indicated, TX-100 extractions were performed at 12°, 22°, or 37°C instead of 4°C.

Filipin staining

Fixed cells were stained with 5 μg/ml filipin as described previously (Neufeld et al., 1999). Filipin fluorescence was quantified from regions of interest containing plasma membrane and underlying cytoplasmic structures using NIH Image.

Cholesterol depletion, loading, and repletion

Solutions for cholesterol depletion, repletion, and loading were made in DME or RPMI supplemented with 25 mM Hepes and 1 mg/ml BSA. For cholesterol depletion, cells were briefly washed, and then incubated in 10 mM MβCD for 30 min at 37°C before TX-100 extraction or FRAP. Cholesterol loading was performed using water-soluble cholesterol (MβCD–cholesterol complexes at ∼6:1 molar ratio; Sigma-Aldrich). Previous work has established that efficient loading of cells occurs when incubated with MβCD–cholesterol complexes prepared at this ratio (Christian et al., 1997; Sheets et al., 1999). MβCD–cholesterol complexes were prepared as a stock solution, 300 mM in MβCD, diluted directly onto the cells to 10 mM in MβCD, and incubated for 30 min at 37°C. Incubation for longer times (1–2 h) led to increased sensitivity to TX-100 extraction in DRM experiments. Cholesterol-loaded cells imaged live for FRAP experiments did not initially exhibit any gross morphological differences from control cells, but over time cells showed a tendency to round up.

References

Anderson, R.G.W., and K. Jacobson. 2002. A role for lipid shells in targeting proteins to caveolae, rafts and other lipid domains. *Science.* 296:1821–1825.

Aroeti, B., and Y.I. Henis. 1988. Effects of fusion temperature on the lateral mobility of Sendai virus glycoproteins in erythrocyte membranes and on cell fusion indicate that glycoprotein mobilization is required for cell fusion. *Biochemistry.* 27:5654–5661.

Bacia, K., I.V. Majoul, and P. Schwille. 2002. Probing the endocytic pathway in live cells using dual-color fluorescence cross-correlation analysis. *Biophys. J.* 83:1184–1193.

Brown, D.A., and J.K. Rose. 1992. Sorting of GPI-anchored proteins to glycolipid-enriched membrane subdomains during transport to the apical cell surface. *Cell.* 68:533–544.

Brown, D.A., and E. London. 1998a. Functions of lipid rafts in biological membranes. *Annu. Rev. Cell Dev. Biol.* 14:111–136.

Brown, D.A., and E. London. 1998b. Structure and origin of ordered lipid domains in biological membranes. *J. Membr. Biol.* 164:103–114.

Bunnell, S.C., D.I. Hong, J.R. Kardon, T. Yamazaki, C.J. McGlade, V.A. Barr, and L.E. Samelson. 2002. T cell receptor ligation induces the formation of dynamically regulated signaling assemblies. *J. Cell Biol.* 158:1263–1275.

Cerneus, D.P., E. Ueffing, G. Posthuma, G.J. Strous, and A. van der Ende. 1993. Detergent insolubility of alkaline phosphatase during biosynthetic transport and endocytosis. Role of cholesterol. *J. Biol. Chem.* 268:3150–3155.

Choudhury, A., M. Dominguez, V. Puri, D.K. Sharma, K. Narita, C.L. Wheatley, D.L. Marks, and R.E. Pagano. 2002. Rab proteins mediate Golgi transport of caveola-internalized glycosphingolipids and correct lipid trafficking in Niemann-Pick C cells. *J. Clin. Invest.* 109:1541–1550.

Choy, E., V.K. Chiu, J. Silletti, M. Feoktistov, T. Morimoto, D. Michaelson, I.E. Ivanov, and M.R. Philips. 1999. Endomembrane trafficking of Ras: the CAAX motif targets proteins to the ER and Golgi. *Cell.* 98:69–80.

Christian, A.E., M.P. Haynes, M.C. Phillips, and G.H. Rothblat. 1997. Use of cyclodextrins for manipulating cellular cholesterol content. *J. Lipid Res.* 38: 2264–2272.

Dietrich, C., L.A. Bagatolli, Z.N. Volovyk, N.L. Thompson, M. Levi, K. Jacobson, and E. Gratton. 2001a. Lipid rafts reconstituted in model systems. *Biophys. J.* 80:1417–1428.

Dietrich, C., Z.N. Volovyk, M. Levi, N.L. Thompson, and K. Jacobson. 2001b. Partitioning of Thy-1, GM1, and crosslinked phospholipid analogs into lipid rafts reconstituted in supported membrane monolayers. *Proc. Natl. Acad. Sci. USA.* 98:10642–10647.

Dietrich, C., B. Yang, T. Fujiwara, A. Kusumi, and K. Jacobson. 2002. Relationship of lipid rafts to transient confinement zones detected by single particle tracking. *Biophys. J.* 82:274–284.

Edidin, M. 1994. Fluorescence photobleaching and recovery, FPR, in the analysis of membrane structure and dynamics. *In* Mobility and Proximity in Biological Membranes. S. Damjanovish, M. Edidin, J. Szollosi, and L. Tron, editors. CRC Press, Boca Raton, FL. 109–135.

Edidin, M. 1996. Getting there is only half the fun. *Current Topics in Membranes.* 43:1–13.

Edidin, M. 2003. The state of lipid rafts: from model membranes to cells. *Annu. Rev. Biophys. Biomol. Struct.* 32:257–283.

Edidin, M., and I. Stroynowski. 1991. Differences between the lateral organization of conventional and inositol phospholipid-anchored membrane proteins. A further definition of micrometer scale membrane domains. *J. Cell Biol.* 112: 1143–1150.

Ellenberg, J., E.D. Siggia, J.E. Moreira, C.L. Smith, J.F. Presley, H.J. Worman, and J. Lippincott-Schwartz. 1997. Nuclear membrane dynamics and reassembly in living cells: targeting of an inner nuclear membrane protein in interphase and mitosis. *J. Cell Biol.* 138:1193–1206.

Feng, B., P.M. Yao, Y. Li, C.M. Devlin, D. Zhang, H.P. Harding, M. Sweeney, J.X. Rong, G. Kuriakose, E.A. Fisher, et al. 2003. The endoplasmic reticulum is the site of cholesterol-induced cytotoxicity in macrophages. *Nat. Cell Biol.* 5:781–792.

Glebov, O.O., and B.J. Nichols. 2004. Lipid raft proteins have a random distribution during localized activation of the T-cell receptor. *Nat. Cell Biol.* 6:238–243.

Grimmer, S., B. van Deurs, and K. Sandvig. 2002. Membrane ruffling and macropinocytosis in A431 cells require cholesterol. *J. Cell Sci.* 115:2953–2962.

Hancock, J.F. 2003. Ras proteins: different signals from different locations. *Nat. Rev. Mol. Cell Biol.* 4:373–384.

Hao, M., S. Mukherjee, and F.R. Maxfield. 2001. Cholesterol depletion induces large scale domain segregation in living cell membranes. *Proc. Natl. Acad. Sci. USA.* 98:13072–13077.

Hering, H., C.C. Lin, and M. Sheng. 2003. Lipid rafts in the maintenance of synapses, dendritic spines, and surface AMPA receptor stability. *J. Neurosci.* 23: 3262–3271.

Hillman, G.M., and J. Schlessinger. 1982. Lateral diffusion of epidermal growth factor complexed to its surface receptors does not account for the thermal sensitivity of patch formation and endocytosis. *Biochemistry.* 21:1667–1672.

Ikonen, E. 2001. Role of lipid rafts in membrane transport. *Curr. Opin. Cell Biol.* 13:470–477.

Ishihara, A., Y. Hou, and K. Jacobson. 1987. The Thy-1 antigen exhibits rapid lateral diffusion in the plasma membrane of rodent lymphoid cells and fibroblasts. *Proc. Natl. Acad. Sci. USA.* 84:1290–1293.

Jacobson, K., and C. Dietrich. 1999. Looking at lipid rafts? *Trends Cell Biol.* 9:87–91.

Jacobson, K., D. O'Dell, and J.T. August. 1984. Lateral diffusion of an 80,000-dalton glycoprotein in the plasma membrane of murine fibroblasts: relationships to cell structure and function. *J. Cell Biol.* 99:1624-33.

Kahya, N., D. Scherfeld, K. Bacia, B. Poolman, and P. Schwille. 2003. Probing lipid mobility of raft-exhibiting model membranes by fluorescence correlation spectroscopy. *J. Biol. Chem.* 278:28109–28115.

Keller, P., D. Toomre, E. Diaz, J. White, and K. Simons. 2001. Multicolour imaging of post-Golgi sorting and trafficking in live cells. *Nat. Cell Biol.* 3:140–149.

Kenworthy, A.K., and M. Edidin. 1998. Distribution of a glycosylphosphatidylinositol-anchored protein at the apical surface of MDCK cells examined at a resolution of <100 Å using imaging fluorescence resonance energy transfer. *J. Cell Biol.* 142:69–84.

Korlach, J., P. Schwille, W.W. Webb, and G.W. Feigenson. 1999. Characterization of lipid bilayer phases by confocal microscopy and fluorescence correlation spectroscopy. *Proc. Natl. Acad. Sci. USA.* 96:8461–8466.

Kusumi, A., and Y. Sako. 1996. Cell surface organization by the membrane skeleton. *Curr. Opin. Cell Biol.* 8:566–574.

Kwik, J., S. Boyle, D. Fooksman, L. Margolis, M.P. Sheetz, and M. Edidin. 2003. Membrane cholesterol, lateral mobility, and the phosphatidylinositol 4,5-bisphosphate-dependent organization of cell actin. *Proc. Natl. Acad. Sci. USA.* 100:13964–13969.

Lange, Y., J. Ye, M. Rigney, and T.L. Steck. 1999. Regulation of endoplasmic reticulum cholesterol by plasma membrane cholesterol. *J. Lipid Res.* 40: 2264–2270.

Lawrence, J.C., D.E. Saslowsky, J.M. Edwardson, and R.M. Henderson. 2003. Real-time analysis of the effects of cholesterol on lipid raft behavior using atomic force microscopy. *Biophys. J.* 84:1827–1832.

Lippincott-Schwartz, J., E. Snapp, and A.K. Kenworthy. 2001. Studying protein dynamics in living cells. *Nat. Rev. Mol. Cell Biol.* 2:444–456.

Lommerse, P.H., G.A. Blab, L. Cognet, G.S. Harms, B.E. Snaar-Jagalska, H.P. Spaink, and T. Schmidt. 2004. Single-molecule imaging of the H-Ras membrane-anchor reveals domains in the cytoplasmic leaflet of the cell membrane. *Biophys. J.* 86:609–616.

Maxfield, F.R. 2002. Plasma membrane microdomains. *Curr. Opin. Cell Biol.* 14: 483–487.

Maxfield, F.R., and D. Wüstner. 2002. Intracellular cholesterol transport. *J. Clin. Invest.* 110:891–898.

Mayor, S., and F.R. Maxfield. 1995. Insolubility and redistribution of GPI-anchored proteins at the cell surface after detergent treatment. *Mol. Biol. Cell.* 6:929–944.

Nehls, S., E.L. Snapp, N.B. Cole, K.J. Zaal, A.K. Kenworthy, T.H. Roberts, J. Ellenberg, J.F. Presley, E. Siggia, and J. Lippincott-Schwartz. 2000. Dynamics and retention of misfolded proteins in native ER membranes. *Nat. Cell Biol.* 2:288–295.

Neufeld, E.B., M. Wastney, S. Patel, S. Suresh, A.M. Cooney, N.K. Dwyer, C.F. Roff, K. Ohno, J.A. Morris, E.D. Carstea, et al. 1999. The Niemann-Pick C1 protein resides in a vesicular compartment linked to retrograde transport of multiple lysosomal cargo. *J. Biol. Chem.* 274:9627–9635.

Nichols, B.J., and J. Lippincott-Schwartz. 2001. Endocytosis without clathrin coats. *Trends Cell Biol.* 11:406–412.

Nichols, B.J., A.K. Kenworthy, R.S. Polishchuk, R. Lodge, T.H. Roberts, K. Hirschberg, R.D. Phair, and J. Lippincott-Schwartz. 2001. Rapid cycling of lipid raft markers between the cell surface and Golgi complex. *J. Cell Biol.* 153:529–541.

Niv, H., O. Gutman, Y. Kloog, and Y.I. Henis. 2002. Activated K-Ras and H-Ras display different interactions with saturable nonraft sites at the surface of live cells. *J. Cell Biol.* 157:865–872.

Orlandi, P.A., and P.H. Fishman. 1998. Filipin-dependent inhibition of cholera toxin: evidence for toxin internalization and activation through caveolae-like domains. *J. Cell Biol.* 141:905–915.

Pelkmans, L., J. Kartenbeck, and A. Helenius. 2001. Caveolar endocytosis of simian virus 40 reveals a new two-step vesicular-transport pathway to the ER. *Nat. Cell Biol.* 3:473–483.

Pralle, A., P. Keller, E.L. Florin, K. Simons, and J.K. Horber. 2000. Sphingolipid-cholesterol rafts diffuse as small entities in the plasma membrane of mammalian cells. *J. Cell Biol.* 148:997–1008.

Prior, I.A., A. Harding, J. Yan, J. Sluimer, R.G. Parton, and J.F. Hancock. 2001. GTP-dependent segregation of H-ras from lipid rafts is required for biological activity. *Nat. Cell Biol.* 3:368–375.

Puri, V., R. Watanabe, M. Dominguez, X. Sun, C.L. Wheatley, D.L. Marks, and R.E. Pagano. 1999. Cholesterol modulates membrane traffic along the endocytic pathway in sphingolipid-storage diseases. *Nat. Cell Biol.* 1:386–388.

Reits, E.A.J., and J.J. Neefjes. 2001. From fixed to FRAP: measuring protein mobility and activity in living cells. *Nat. Cell Biol.* 3:E145–E147.

Rietveld, A., and K. Simons. 1998. The differential miscibility of lipids as the basis for the formation of functional membrane rafts. *Biochim. Biophys. Acta.* 1376:467–479.

Rodal, S.K., G. Skretting, O. Garred, F. Vilhardt, B. van Deurs, and K. Sandvig. 1999. Extractions of cholesterol with methyl-β-cyclodextrin perturbs formation of clathrin-coated endocytic vesicles. *Mol. Biol. Cell.* 10:961–974.

Rothberg, K.G., J.E. Heuser, W.C. Donzell, Y.S. Ying, J.R. Glenney, and R.G. Anderson. 1992. Caveolin, a protein component of caveolae membrane coats. *Cell.* 68:673–682.

Saffman, P.G., and M. Delbrück. 1975. Brownian motion in biological membranes. *Proc. Natl. Acad. Sci. USA.* 72:3111–3113.

Samsonov, A.V., I. Mihalyov, and F.S. Cohen. 2001. Characterization of cholesterol-sphingomyelin domains and their dynamics in bilayer membranes. *Bio-

phys. J. 81:1488–1500.

Saxton, M.P. 1999. Lateral diffusion of lipids and proteins. *Current Topics in Membranes.* 48:229–282.

Scheiffele, P., M.G. Roth, and K. Simons. 1997. Interaction of influenza virus haemagglutinin with sphingolipid-cholesterol membrane domains via its transmembrane domain. *EMBO J.* 16:5501–5508.

Schütz, G.J., G. Kada, V.P. Pastushenko, and H. Schindler. 2000. Properties of lipid microdomains in a muscle cell membrane visualized by single molecule microscopy. *EMBO J.* 19:892–901.

Severs, N.J. 1997. Cholesterol cytochemistry in cell biology and disease. *Subcell. Biochem.* 28:477–505.

Sheets, E.D., R. Simson, and K. Jacobson. 1995. New insights into membrane dynamics from the analysis of cell surface interactions by physical methods. *Curr. Opin. Cell Biol.* 7:707–714.

Sheets, E.D., G.M. Lee, R. Simson, and K. Jacobson. 1997. Transient confinement of a glycosylphosphatidylinositol-anchored protein in the plasma membrane. *Biochemistry.* 36:12449–12458.

Sheets, E.D., D. Holowka, and B. Baird. 1999. Critical role for cholesterol in Lyn-mediated tyrosine phosphorylation of FcεRI and their association with detergent-resistant membranes. *J. Cell Biol.* 145:877–887.

Shvartsman, D.E., M. Kotler, R.D. Tall, M.G. Roth, and Y.I. Henis. 2003. Differently anchored influenza hemagglutinin mutants display distinct interaction dynamics with mutual rafts. *J. Cell Biol.* 8:879–888.

Siggia, E.D., J. Lippincott-Schwartz, and S. Bekiranov. 2000. Diffusion in inhomogeneous media: theory and simulations applied to whole cell photobleach recovery. *Biophys. J.* 79:1761–1770.

Simons, K., and E. Ikonen. 1997. Functional rafts in cell membranes. *Nature.* 387:569–572.

Simons, K., and D. Toomre. 2000. Lipid rafts and signal transduction. *Nat. Rev. Mol. Cell Biol.* 1:31–41.

Simons, K., and R. Ehehalt. 2002. Cholesterol, lipid rafts, and disease. *J. Clin. Invest.* 110:597–603.

Skibbens, J.E., M.G. Roth, and K.S. Matlin. 1989. Differential extractability of influenza hemagglutinin during intracellular transport in polarized epithelial cells and nonpolar fibroblasts. *J. Cell Biol.* 108:821–832.

Subczynski, W.K., and A. Kusumi. 2003. Dynamics of raft molecules in the cell and artificial membranes: approaches by pulse EPR spin labeling and single molecule optical microscopy. *Biochim. Biophys. Acta.* 1610:231–243.

Subtil, A., I. Gaidarov, K. Kobylarz, M. Lampson, J. Keen, and T. McGraw. 1999. Acute cholesterol depletion inhibits clathrin-coated pit budding. *Proc. Natl. Acad. Sci. USA.* 96:6775–6780.

Sugimoto, Y., H. Ninomiya, Y. Ohsaki, K. Higaki, J.P. Davies, Y.A. Ioannou, and K. Ohno. 2001. Accumulation of cholera toxin and GM1 ganglioside in the early endosome of Niemann-Pick C1-deficient cells. *Proc. Natl. Acad. Sci. USA.* 98:12391–12396.

Suzuki, K., and M.P. Sheetz. 2001. Binding of cross-linked glycosylphosphatidylinositol-anchored proteins to discrete actin-associated sites and cholesterol-dependent domains. *Biophys. J.* 81:2181–2189.

Tabas, I. 2002. Consequences of cellular cholesterol accumulation: basic concepts and physiological implications. *J. Clin. Invest.* 110:905–911.

Thomsen, P., K. Roepstorff, M. Stahlhut, and B. van Deurs. 2002. Caveolae are highly immobile plasma membrane microdomains, which are not involved in constitutive endocytic trafficking. *Mol. Biol. Cell.* 13:238–250.

Toomre, D., P. Keller, J. White, J.-C. Olivo, and K. Simons. 1999. Dual-color visualization of trans-Golgi network to plasma membrane traffic along microtubules in living cells. *J. Cell Sci.* 112:21–33.

Toomre, D., J.A. Steyer, P. Keller, W. Almers, and K. Simons. 2000. Fusion of constitutive membrane traffic with the cell surface observed by evanescent wave microscopy. *J. Cell Biol.* 149:33–40.

Vrljic, M., S.Y. Nishimura, S. Brasselet, W.E. Moerner, and H.M. McConnell. 2002. Translational diffusion of individual Class II MHC membrane proteins in cells. *Biophys. J.* 83:2681–2692.

Wey, C.L., R.A. Cone, and M.A. Edidin. 1981. Lateral diffusion of rhodopsin in photoreceptor cells measured by fluorescence photobleaching and recovery. *Biophys. J.* 33:225–232.

Zaal, K.J.M., C.L. Smith, R.S. Polishchuk, N. Altan, N.B. Cole, J. Ellenberg, K. Hirschberg, J.F. Presley, T.H. Roberts, E. Siggia, et al. 1999. Golgi membranes are absorbed into and reemerge from the ER during mitosis. *Cell.* 99:589–601.

Zacharias, D.A., J.D. Violin, A.C. Newton, and R.Y. Tsien. 2002. Partitioning of lipid-modified monomeric GFPs into membrane microdomains of live cells. *Science.* 296:913–916.

Zhang, F., B. Crise, B. Su, Y. Hou, J.K. Rose, A. Bothwell, and K. Jacobson. 1991. Lateral diffusion of membrane-spanning and glycosylphosphatidylinositol-linked proteins: toward establishing rules governing the lateral mobility of membrane proteins. *J. Cell Biol.* 115:75–84.

Zhang, W., J. Sloan-Lancaster, J. Kitchen, R.P. Trible, and L.E. Samelson. 1998a. LAT: the ZAP-70 tyrosine kinase substrate that links T cell receptor to cellular activation. *Cell.* 92:83–92.

Zhang, W.G., R.P. Trible, and L.E. Samelson. 1998b. LAT palmitoylation: its essential role in membrane microdomain targeting and tyrosine phosphorylation during T cell activation. *Immunity.* 9:239–246.